Electronic Supplementary Material (ESI) for CrystEngComm.

Electronic Supporting Information

for

Inter-diffusion of Cu^{2+} Ions to CuS Nanocrystals and the Confinement Effect on Microwave Absorption Properties

Jiani Gu[a], Yi Xie[a*], Wenhui Chen[a], Chao Hu[a], Zhiyuan Xu[b], Fen Qiao[c], Xiaoqing Liu[d], Xiujian Zhao[a], Gaoke Zhang[a*]

[a] *State Key Laboratory of Silicate Materials for Architectures, Wuhan University of Technology (WUT), No. 122, Luoshi Road, Wuhan 430070, P. R. China*

[b] *School of Energy & Power Engineering, Jiangsu University, Zhenjiang, 212013, P. R. China*

[c] *State Key Laboratory of Advanced Technology for Materials Synthesis and Processing, Wuhan University of Technology (WUT), No. 122, Luoshi Road, Wuhan 430070, P. R. China*

[d] *Center for Materials Research & Testing, Wuhan University of Technology, Wuhan, Hubei 430070, P.R. China*

Email: xiey@whut.edu.cn; gkzhang@whut.edu.cn

1. Characterization of $Cu_{2-x}S$ NCs achieved by reacting CuS with different amounts of Cu^{2+}

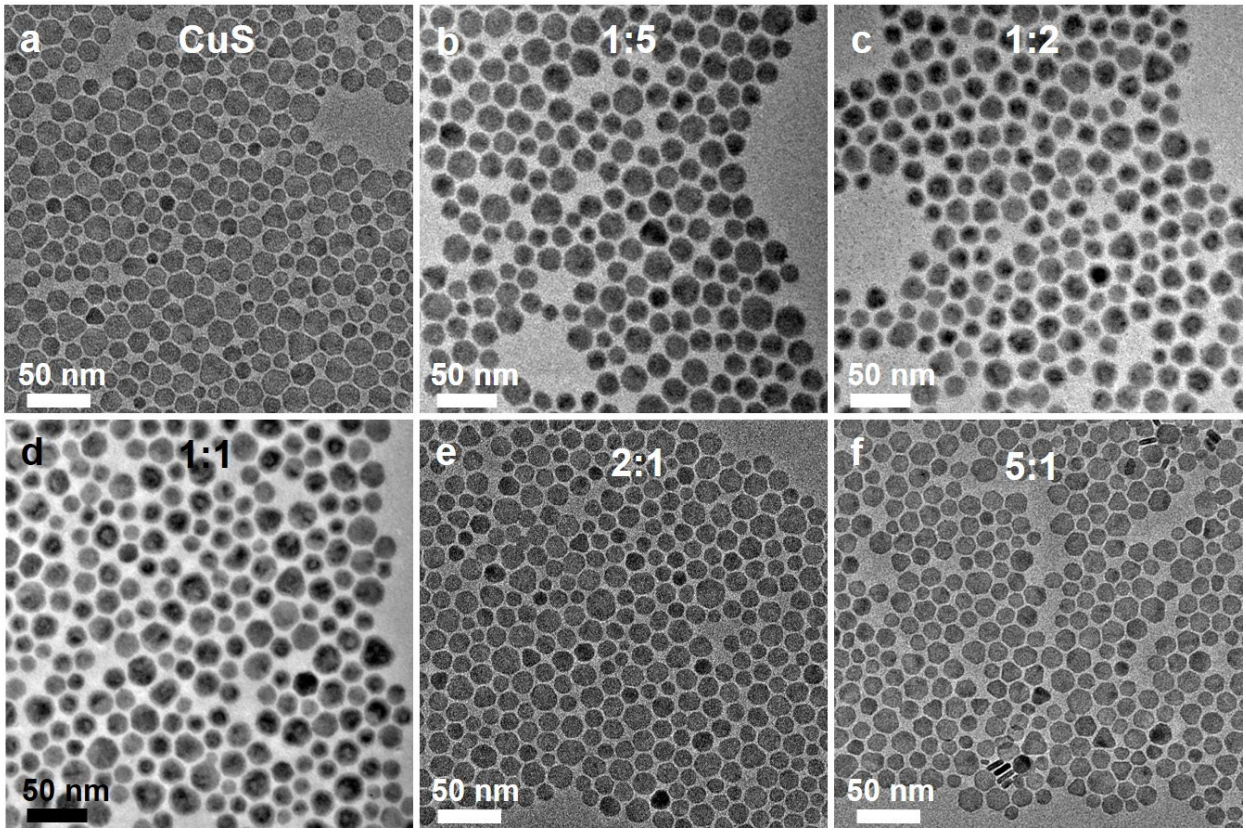

Fig. S1 *(a) TEM images of the as-synthesized CuS nanoplates by heat-up procedure. (b-f) TEM images of $Cu_{2-x}S$ NCs collected by reacting the as-synthesized CuS NCs with Cu^{2+} ions, varying the precursor molar ratios of the Cu^{2+} in $CuCl_2$ to the Cu^{+} in CuS (denoted as Cu^{2+}:Cu^{+}) as dictated, in the presence of mild reducing agent, ascorbic acid (AA).*

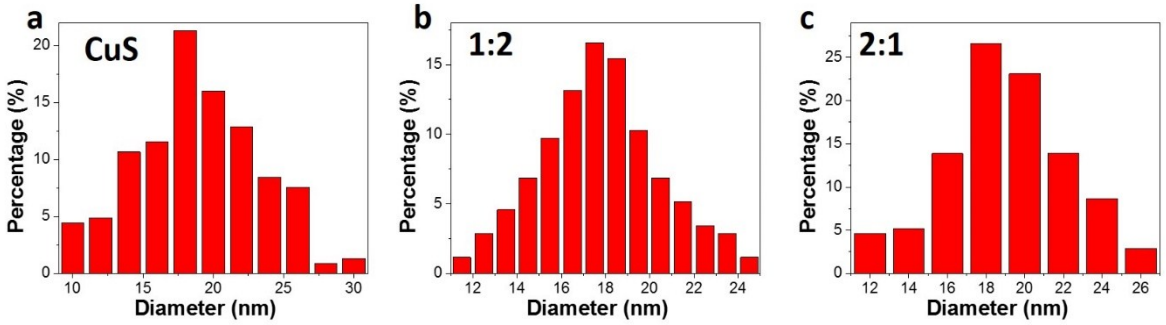

Fig. S2 *Size (in diameter) distribution histogram for the various $Cu_{2-x}S$ nanoplates obtained by reacting the as-synthesized CuS NCs with Cu^{2+} in the presence of different precursor Cu^{2+}:Cu^{+} molar ratios as dictated. The average diameter of these typical samples are calculated to be*

18.0 ± 2.5 nm, 18.1 ± 2.6 nm, and 18.1 ± 3.0 nm, respectively. The overall particle sizes can be retained.

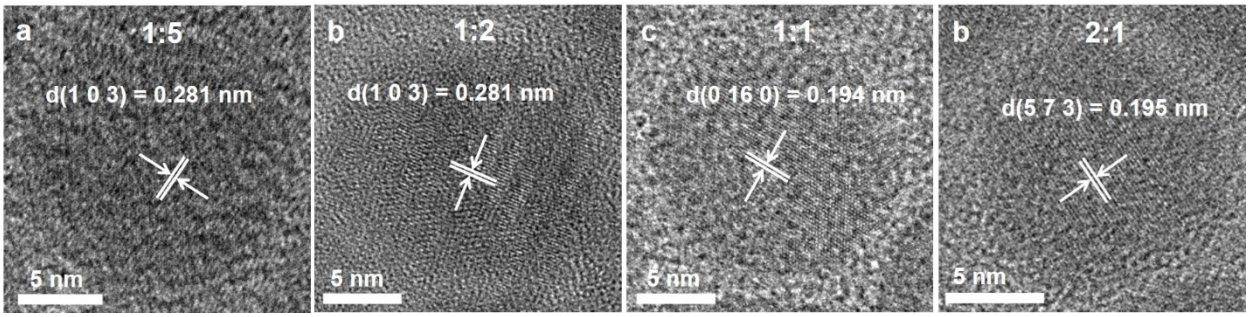

Fig. S3 *HRTEM images of $Cu_{2-x}S$ NCs collected by reacting the as-synthesized CuS NCs with Cu^{2+} in the presence of different precursor Cu^{2+}:Cu^{+} molar ratios as dictated. The lattice spacing shown from panels a-d) can be respectively assigned to the (103), (103), (0160) and (573) planes of covellite (a-b), roxbyite (c) and chalcocite (d) phases.*

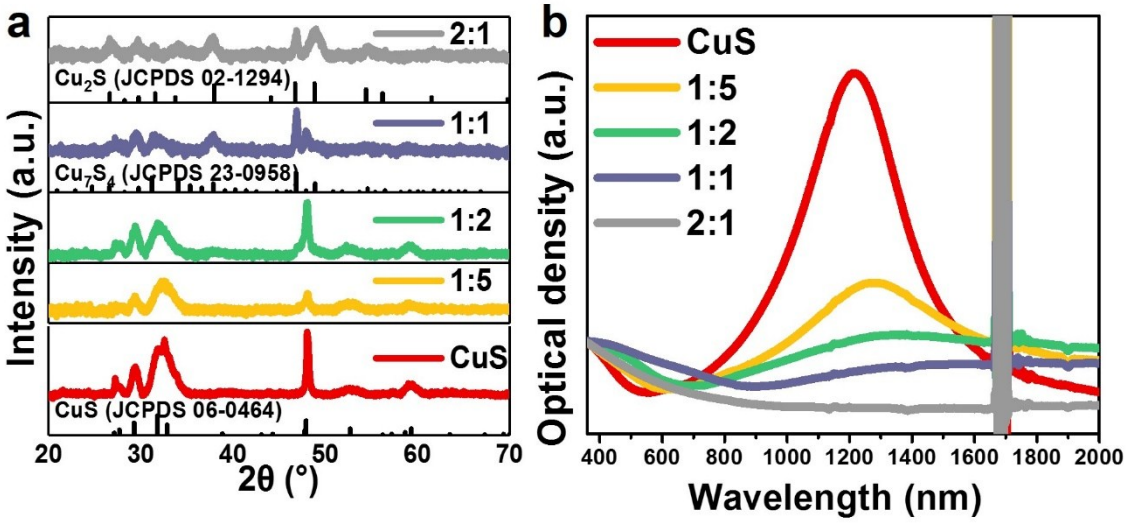

Fig. S4 *XRD patterns (a) and optical absorbance (b) of the various $Cu_{2-x}S$ nanoplates achieved by reacting the as-synthesized CuS NCs with with Cu^{2+} ions in the presence of different precursor Cu^{2+}:Cu^{+} precursor ratios as dictated. For comparison, the standard XRD patterns of covellite (CuS, JCPDS No. 06-0464), roxbyite (Cu_7S_4, JCPDS No. 23-0958) and chalcocite (Cu_2S, JCPDS No. 02-1294) are provided in panel a). The precursor Cu^{2+}:Cu^{+} ratios play a critical role in controlling the structure and the optical properties of the final samples, as evidenced by the evolution of*

XRD patterns and optical spectra. The characterization and analysis confirm that the as-synthesized CuS nanoplates display well-defined NIR plasmon absorbance centered at around 1209 nm. However, the NIR plasmon absorbance damped and vanished with increasing the precursor Cu^{2+}:Cu^{+} molar ratios.

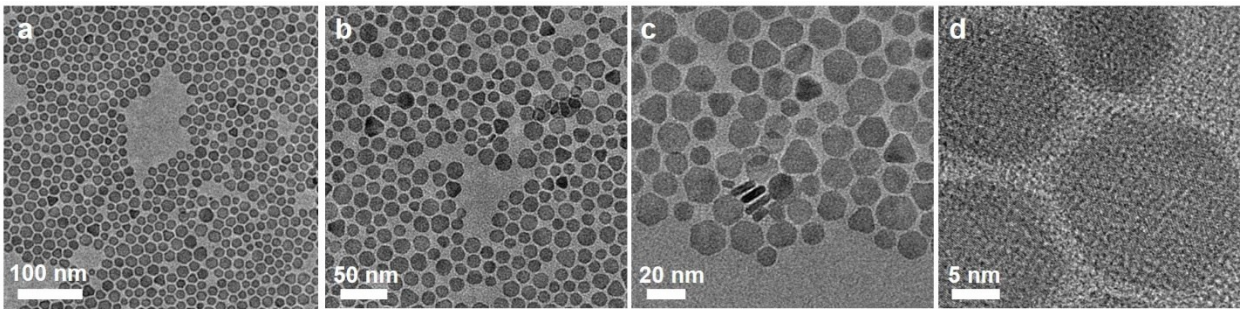

Fig. S5 *Representative TEM images of different magnifications of $Cu_{2-x}S$ NCs achieved by reacting CuS with Cu^{2+} ions in the presence of AA. The TEM/HRTEM measurements were performed with a field emission gun working at 200 kV accelerating voltage.*

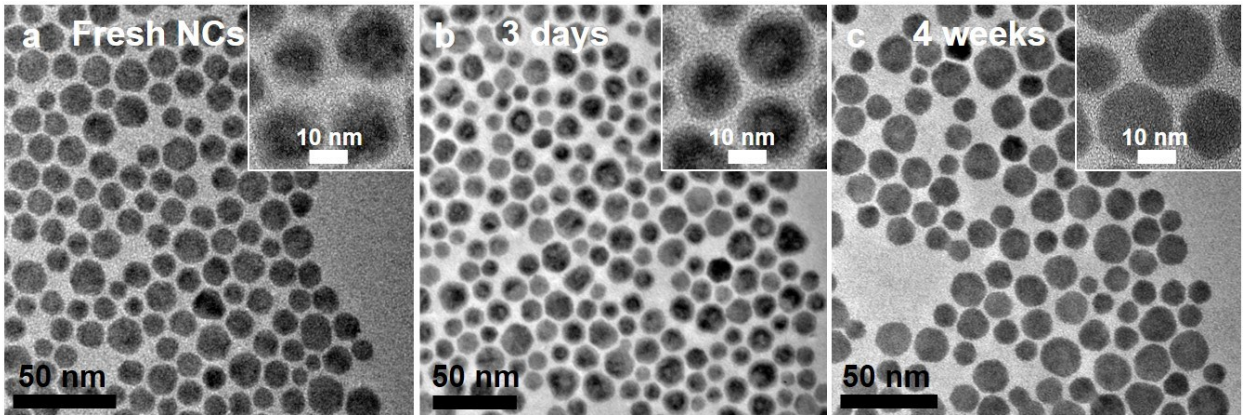

Fig. S6 *The TEM images of the as-synthesized fresh CuS@$Cu_{2-x}S$ core-shell NCs (a) and the same sample stored in toluene solvent for 3 days (b) and 4 weeks (c), respectively. The TEM/HRTEM measurements were performed with a field emission gun working at 100 kV accelerating voltage.*

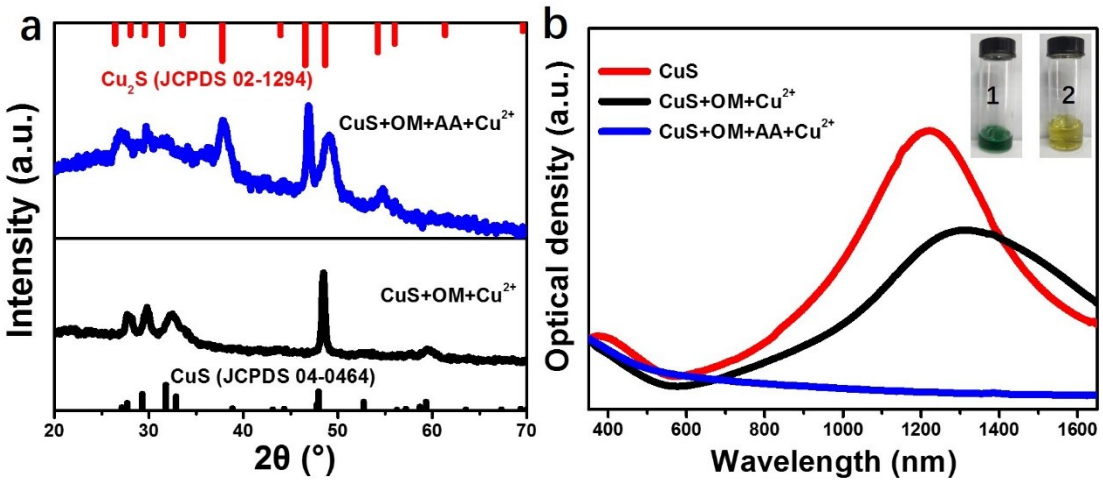

Fig. S7 *The XRD patterns (a) and optical spectra (b) of the as-synthesized CuS, and NCs collected in the presence of OM alone (black curves), and of both AA and OM (the blue curves). The photos of the supernatant collected after centrifugation in the presence of OM alone (No. 1 of the insets in panel b), and of both AA and OM (No. 2 of the insets in panel b) are also provided.*

2. Characterization of $Cu_{2-x}S$ NCs collected at different time by reacting CuS NCs with Cu^{2+} ions

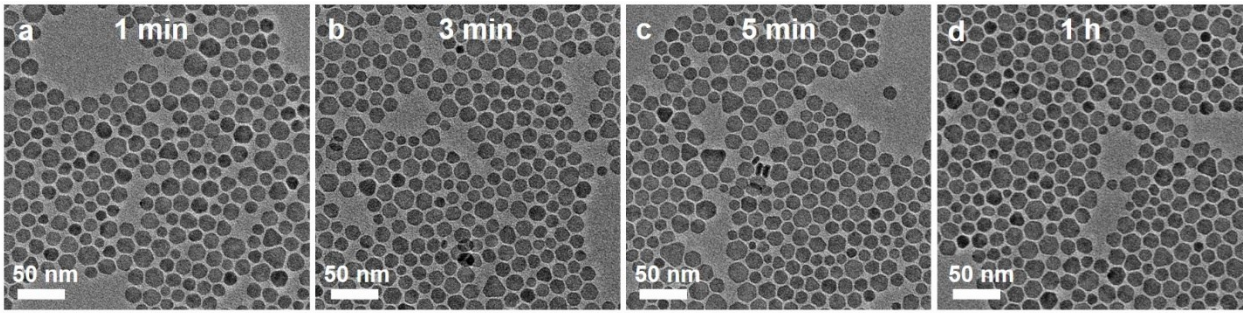

Fig. S8 *The evolution of TEM images (a-d) of the various $Cu_{2-x}S$ NCs collected at different time as dictated, by reacting CuS NCs with Cu^{2+} in the presence of AA. The precursor Cu^{2+}:Cu^{+} molar ratio is 2:1.*

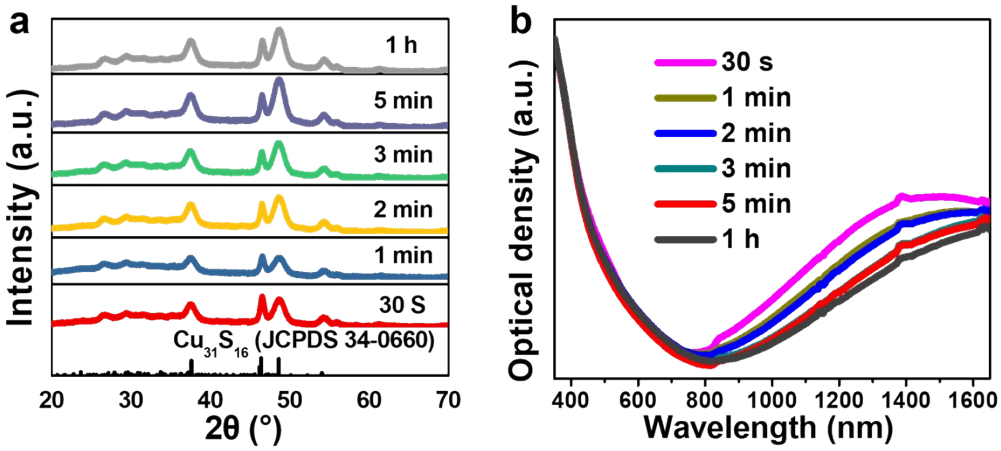

Fig. S9 *XRD patterns (a) and optical absorbance (b) of the various $Cu_{2-x}S$ NCs collected at different time as dictated, by reacting CuS NCs with Cu^{2+} in the presence of AA. The precursor Cu^{2+}:Cu^{+} molar ratio is 3:2. For comparison, the standard XRD pattern of chalcocite ($Cu_{31}S_{16}$, JCPDS No.34-0660) is provided in panel a).*

3. Microwave absorption properties of various $Cu_{2-x}S$/paraffin composites

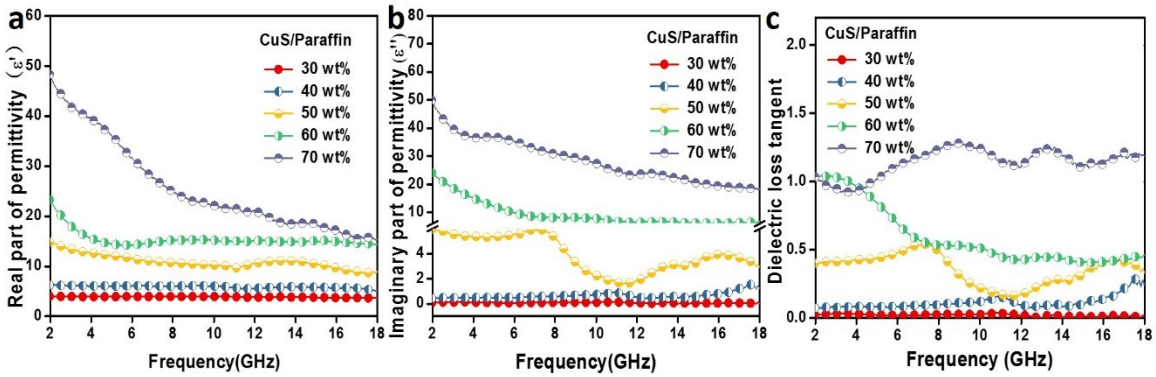

Fig. S10 *Frequency dependence on real permittivity (a), imaginary permittivity (b) and dielectric loss tangent (c) of the CuS/paraffin composites with different CuS NCs loadings as dictated.*

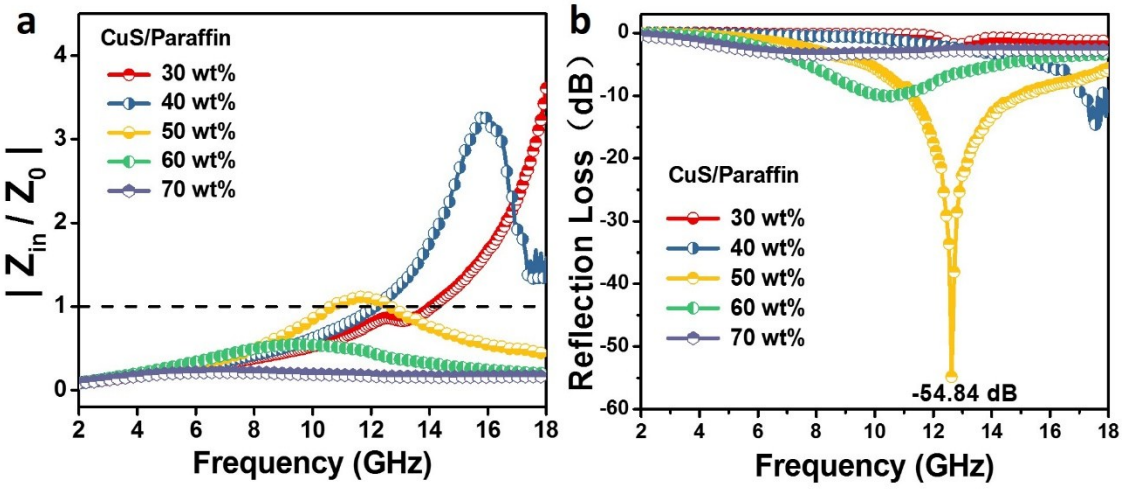

Fig. S11 *The normalized impedance (a) and microwave reflection losses (b) of the CuS/paraffin composites with different CuS loadings at certain thickness of 1.95 mm in the frequency range of 2-18 GHz.*

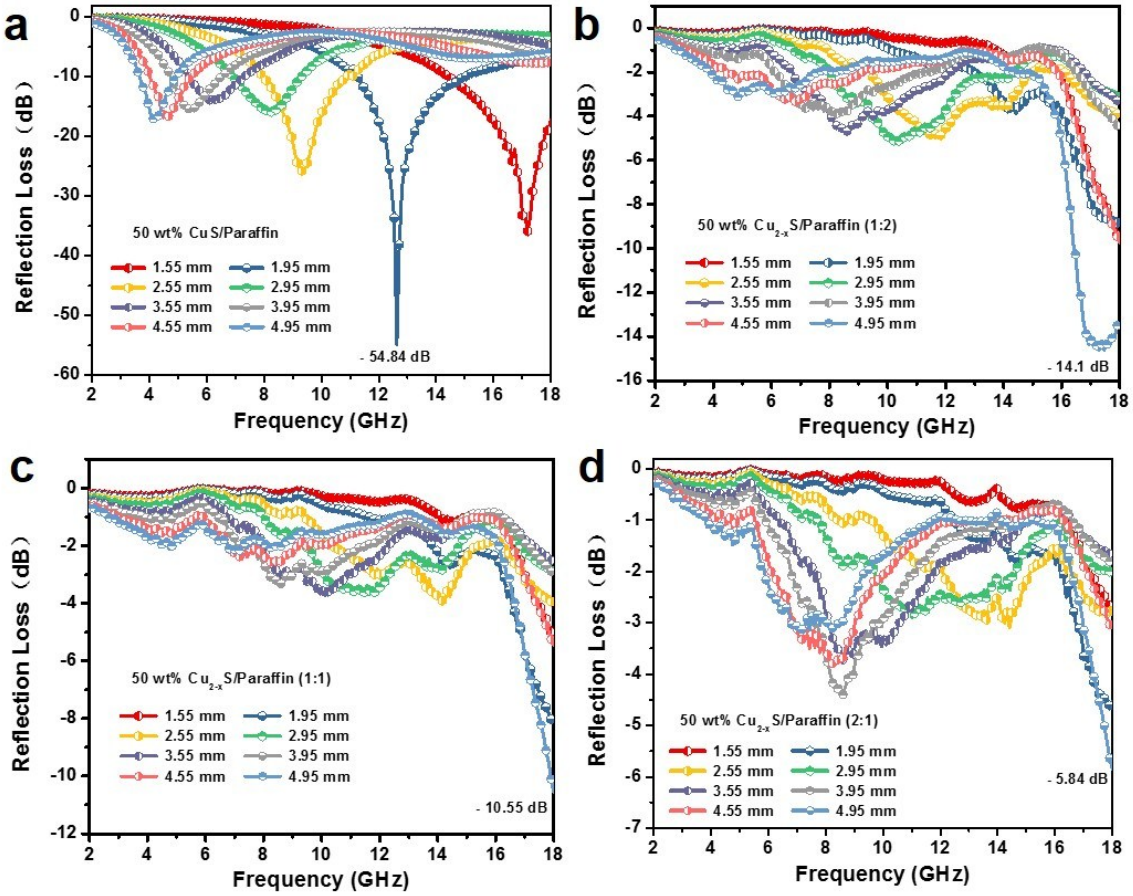

Fig. S12 *The microwave reflection losses with various thicknesses of 50 wt% $Cu_{2-x}S$/paraffin composites in the frequency range of 2-18 GHz. The $Cu_{2-x}S$ NCs were achieved by reacting CuS NCs with Cu^{2+}, in the presence of different precursor Cu^{2+}:Cu^{+} precursor ratios as dictated in each panel.*

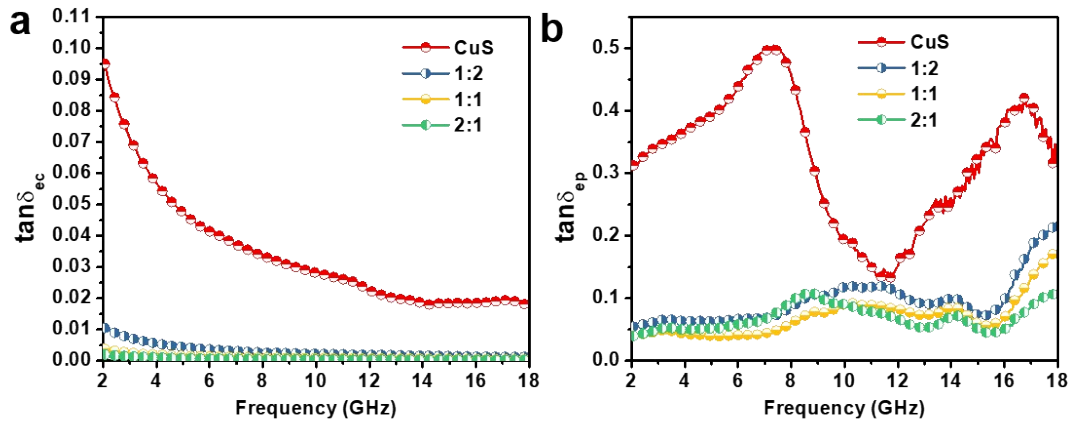

Fig. S13 *Loss tangent $tan\delta_{ec}$ (a) and $tan\delta_{ep}$ (b) of 50 wt% $Cu_{2-x}S$/paraffin composites in the frequency range of 2-18 GHz. The $Cu_{2-x}S$ NCs were achieved by reacting CuS NCs with Cu^{2+}, in the presence of different precursor Cu^{2+}:Cu^{+} molar ratios as dictated.*

Table S1. *The microwave absorbing properties of the CuS/paraffin and the various $Cu_{2-x}S$/paraffin composites. The $Cu_{2-x}S$ NCs are achieved by reacting CuS NCs with different amounts of Cu^{2+} cations (denoted as precursor Cu^{2+}:Cu^{+} ratios as dictated in the first column). The loading in all cases is 50 wt %.*

Samples	***RL* (dB)**	***f_r* (GHz)**	**Absorption bandwidth (GHz)**		**Thickness d (mm)**
			<-8 dB	**<-10 dB**	
CuS	-54.84	12.63	5.6	3.8	1.95
	-42.91	8.96	3.9	2.7	2.65
$Cu_{2-x}S$（1:2）	-20.63	16.84	>2	>1.9	5.1
$Cu_{2-x}S$（1:1）	-14.42	18	>1	>0.6	5.1
$Cu_{2-x}S$（2:1）	-7.812	18	-	-	5.1

4. Calculation of free carrier (hole) density in the various NCs

According to the Drude model, the frequency w_{LSPR} of the localized surface plasmon resonance can be described as: [1-2]

$$W_{LSPR} = \sqrt{\frac{w_p^2}{1+2\varepsilon_m} - \gamma^2}$$

Where γ represents the line width of the plasmon resonance band, ε_m is the dielectric constant of the environment surrounding the NCs (ε_m = 2.38 for toluene) and w_p is the plasma frequency. The w_{LSPR} and γ can be calculated from the experimental spectrum (see Fig. S5b). The relationship between bulk plasma frequency (w_p) and free carrier density (N_h) is:

$$W_P = \sqrt{\frac{N_h e^2}{\varepsilon_0 m_h}}$$

where m_h is the hole effective mass, approximated as $0.8m_0$ (where m_0 is the electron mass), and e is the electron charge. From the above Eq., the N_h for the as-synthesized covellite NCs and the various $Cu_{2-x}S$ NCs can be estimated and summarized in Table S2.

Table S1 *The summary on the free carriers (holes) density of the as-synthesized covellite CuS and the various $Cu_{2-x}S$ NCs prepared by reacting CuS NCs with Cu^{2+} ions in the presence of different starting Cu^{2+}:Cu^{+} molar ratios as dictated.*

Samples	**N_h (cm^{-3})**
CuS	3.863×10^{21}
$Cu_{2-x}S$ (1:2)	3.262×10^{21}
$Cu_{2-x}S$ (1:1)	2.328×10^{21}
$Cu_{2-x}S$ (2:1)	0

References

[1] J. M. Luther, P. K. Jain, T. Ewers and A. P. Alivisatos, *Nat. Mater.* **2011**, *10*, 361-366.

[2] Y. Xie, A. Riedinger, M. Prato, A. Casu, A. Genovese, P. Guardia, S. Sottini, C. Sangregorio, K. Miszta, S. Ghosh, T. Pellegrino and L. Manna, *J. Am. Chem. Soc.* **2013**, *135*, 17630-17637.